Dear Editor:

Thank you very much for your email dated October 10, 2025, which reminded us of another referee's report on the SciPost Website and also requested our manuscript for major revisions.

In general, the referee 2 thought that our results on supercurrent-VP coupling and their effect on SDE is interesting, our findings were not proposed in previous work. However, the referee 2 also raised questions about the logic and validity of some assumptions in our theoretical framework, and provided constructive suggestions for further improvement. We appreciate the referee's helpful comments. In response to his/her report, we have attached a point-to-point response below. According to our replies to reports of referee 1 and referee 2, we have made corresponding revisions of our manuscript and denoted the main changes by red color in the revised maniscript. The main changes are as follows:

1) We revised the Fig. 1 and Fig. 3 to make our theory more clear.
2) We add some explanations in 2nd, 3rd and 4th paragraphs of Page 7 to illustrate the logic of our theory to determine actual critical currents.
3) We add a new appendix (Appendix. C) with a new figure (Fig. 7) to discuss the effect of trigonal warping.
4) We add a new appendix (Appendix. D) with a new figure (Fig. 8) to discuss the coupling between supercurrents and valley polarizations.
5) We add some discussions about the estimation of $\alpha_{\pm}$ in a more realistic tight-binding model in Appendix. E with a new figure (Fig. 9).
6) We add some statements in the section of 'Discussions and conclusion' to emphasis some correspondences between our theoretical calculations and experimental observations.
7) Some new references are cited, see Refs. 4, 28, 29, 40, 80-85.

With these modifications, we resubmit this manuscript to SciPost Physics for further consideration.

Yours sincerely

Yu-Chen Zhuang and Qing-Feng Sun

==========

Response to Report # 2 by Anonymous (Referee 2)

==========

We are very grateful for Referee 2 of reviewing our work and giving a valuable report. Below we present our reply to the referee's comments and suggestions. The corresponding revisions are also made in our modified manuscript.

Comment:

The manuscript considers effect of current-induced valley polarization (VP) on superconducting diode effect (SDE), in mean-field toy model. Main emphasis is on dependence of VP on the applied (super)currents and its implications on SDE.

How charge current influences VP in normal state has been discussed in several previous works eg [49], and similarly for how VP influences SDE eg [57]. The discussion here attempts to put these two together phenomenologically. It appears previous works do not consider the mechanism on SDE discussed here.

The current-VP coupling is described by Eqs. (4,5), which are argued to hold in normal state, similar to Ref. [49]. It is not shown in the text they are valid with same coefficients in superconducting state. The argument why this would not matter appears not rigorous but important for conclusions (see detailed point 1).

Consequences of this assumption are then explored in fairly straightforward calculations within a simple model with some electron dispersion, with several numerical results in Sec 3.

In principle, the results on supercurrent-VP coupling and their effect on SDE is interesting, even though it is not demonstrated in this work this mechanism is relevant for some specific realistic system. The main results however appear to hinge on an assumption whose validity is not clear and sufficiently explored in the text. If this question can be clarified, the results may be suitable for publication.

Reply: We thank the referee for the insightful comments on our manuscript. Next, we will respond to the questions and suggestions raised by the referee one by one.

Comment **1**:

1 - On p. 7 line 204: The argumentation for Eqs. (4,5) discusses only nonequilibrium normal (N) state, and its validity is not shown for the superconducting (S) state.

It is asserted in the text that this does not matter, arguing one can approach the transition from the normal side. This appears to still implicitly assume that VP is continuous across the S/N transition. However, at the critical current on the S-side the order parameter Delta has a nonzero finite value, whereas the N-side one is in nonequilibrium state with different Delta, so it's not clear why the assumption would work.

Generally, Eqs. (4,5), the critical current, and the SDE should be found from the same

equilibrium free energy. There, if e.g. VP changes discontinuously in current-carrying S/N transition, the transition point cannot be seen from Fig. 1(b) by approaching from the "normal" region and does not need to lie on the $\tilde{j}_c$ line in the figure.

I think the discussion in the manuscript is not rigorous enough on this point. As the qualitative and quantitative main results rely on this, a more complete argument should be presented, eg. a consistent equilibrium model would improve the manuscript.

Reply: We thank the referee for the thoughtful comments. We will explain this point from two aspects.

(1) In the normal phase, the applied current j_{ext} with a finite electric voltage V induces a nonequilibrium electron distribution and modulates the valley polarization according to Fig. 1(a). While in the superconducting phase, the system returns to equilibrium and the voltage-induced nonequilibrium electron occupations cannot appear. Although the physical picture in Fig. 1(a) is indeed not valid in superconducting phases, **we emphasis that our theory of the actual critical currents j_c is reasonable to describe a current-driven phase transition from the normal phase into the superconducting phase.**

For clearly demonstrate our logic, we made some modifications to the original Fig. 1 (See Fig. R1). In Fig. R1(b), we distinguish the normal phases and superconducting phases by magenta solid lines and cyan dashed lines. Like Fig. 3 in the main text, we also add some magenta arrows on $h_v - j_{ext}$ lines to demonstrate **that our theory focuses on phase transitions process where normal states are driven into the superconducting states.** To explain the rationality of this phase transition, we take the evolution from point A to point B as an example. At point A, due to a very large initial valley splitting h_v^0, the system stays in the normal state. As the applied current j_{ext} increases, the valley splitting h_v will be quickly reduced according to the $h_v - j_{ext}$ relation. However, before arriving at point B (along the magenta solid lines), the applied current J_{ext} keeps larger than the corresponding intrinsic depairing currents $\tilde{j}_{c+}(h_v)$ (red and blue solid lines) that the superconducting phase can carry. Therefore, the system remains in the normal phase from point A to point B, and our theory is explicit in this process. A critical change happens when the applied current j_{ext} passes through the intersection point B. **If we assume that the system still keeps in the normal phase after point B, the valley splitting field h_v has to continue to weaken by the normal current j_{ext} along $h_v - j_{ext}$ relation (cyan dashed line). At this time, the corresponding intrinsic depairing currents $\tilde{j}_{c+}(h_v)$ will exceed the J_{ext}, meaning that the normal phase is actually unstable. This paradox directly refutes the original assumption, implying that the superconducting phase is, in fact, more favored after crossing the point B. Therefore, it is reasonable to denote the intersection point B as the actual critical current for the transition process from the normal phase to the superconducting phase.**

The referee may doubt that VP changes discontinuously in current-carrying S/N transition. However, such a discontinuous change of VP is itself natural. **Similarly, when a system undergoes a superconducting phase transition by varying the electric**

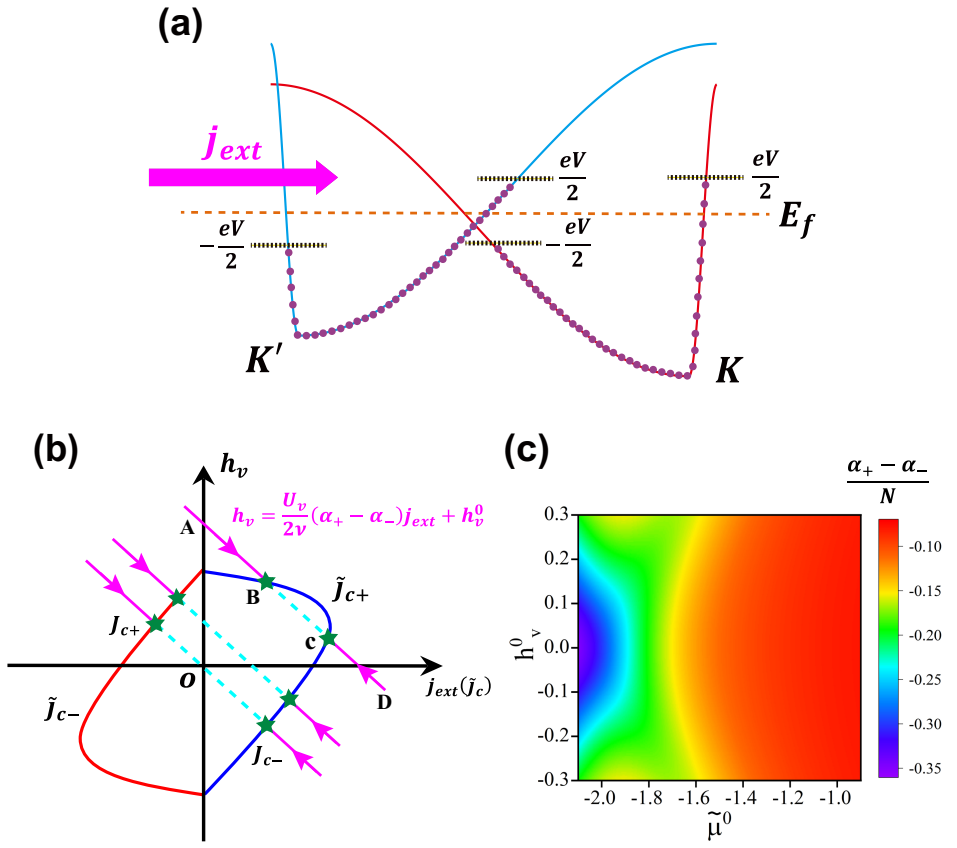

FIG. R1: (a) Schematic illustration of the current-induced valley polarization modulation. The red and blue solid line denote two effective valley bands with the index $\tau = \pm$ (i.e., K, K'). The purple dots denote the occupied electrons on each band. Once an electric current j_{ext} (magenta arrow line) is applied, the local Fermi level for electrons with positive (negative) group velocities will climb (descend) by $eV/2$ relative to Fermi level E_f in equilibrium (black dashed lines). (b) The red and dark blue solid lines respectively denote intrinsic depairing currents $\tilde{j}_{c\pm}$ versus the valley splitting field h_v. The magenta solid lines and cyan dashed lines denote several $h_v - j_{ext}$ relations of Eq. (5) with different h_v^0 (intersections with the vertical axis). At magenta solid lines, the system stays in the normal phase. While for cyan dashed lines, the system has entered the superconducting phase. The magenta arrows denote the direction of the phase transition starting from the normal phase to the superconducting phase, which is the focus of our theory. The intersection points (dark green stars) denote predicted actual critical currents $j_{c\pm}$. (c) The colormap for $(\alpha_+ - \alpha_-)/N$ versus h_v^0 and $\tilde{\mu}^0$.

current, many experiments have also shown that the electric voltage could experience an abrupt change after crossing the transition point [Nano Lett. 21, 216 (2020), Nat. Commun. 16, 531 (2025)]. From the normal state to the superconducting state, the electric voltage will suddenly drop from a finite value to zero. In addition, the discontinuity of h_v making the $h_v - j_{ext}$ line and $\tilde{j}_c$ in B-C part not invalid will not influence the logic and judgement we discussed above. It is only about current behaviors after the system completes the superconducting phase transition. Our theory aims to demonstrate that as long as the system stays in normal phases from point A

to cross point B, the normal phases should be unstable.

(2) On the other hand, although the physical picture in Fig. R1(a) is invalid in superconducting phases, it does not means the valley polarization holds unchanged in cyan regions. **Actually, analogous to normal currents, the supercurrents can also couple to h_v.**

In detail, when the system enters the superconducting phase, the supercurrent j_s is no longer driven by the finite electric voltage but instead carried by finite-momentum Cooper pairs. In other words, the coupling between the valley polarization and supercurrents is equal to discuss the influences of the Cooper-pair momentum $2q$ and the superconducting order parameter Δ on h_v. To investigate this effect, we simultaneously consider the inter-valley repulsive interaction and inter-valley superconducting pairing, and treat them together within a mean-field approximation [Phys. Rev. Lett. **132**, 046003 (2024)]. Thereby, the total free energy F_t should be a combination of free energies in Eq. (2) and Eq. (8) in the main text and is now a function of two order parameters $\Delta(q)$, h_v and the momentum q:

$$F_t(q,\Delta(q),h_v) = -T\sum_{k,\eta=\pm}\ln(1+e^{-\frac{\tilde{E}_\eta(k,q)}{T}})+\sum_k E_{-k+q,-}+\frac{\mathcal{V}\Delta(q)^2}{U_s}+\frac{\mathcal{V}h_v^2}{U_v}-\frac{U_v}{\mathcal{V}}n^2+\mu n \quad \text{(R1)}$$

Note that the parameters in Eq. (R1) coincide with those in Eq. (2) and Eq. (8) in the main text. $\tilde{E}_\pm$ are the eigen-energies for the BdG Hamiltonian of Eq. (6). n and μ denote the total electron number $n=\sum_{k,\tau}\langle c^\dagger_{k,\tau}c_{k,\tau}\rangle$ and the chemical potential of the system, respectively. For simplicity, we here set them as constants which will not influence the total free energy.

To keep the system in the minimum point of the total free energy, we demand that the first-order derivatives of F_t with respect to h_v and Δ are both zero for the fixed q. These lead to a set of self-consistent equations:

$$\begin{cases}\frac{\partial F_t(q,\Delta,h_v)}{\partial h_v}=0,\\ \frac{\partial F_t(q,\Delta,h_v)}{\partial \Delta}=0,\end{cases}\Rightarrow\begin{cases}h_v(\Delta,q)=\frac{U_v}{2\mathcal{V}}\sum_k\left[f(\tilde{E}_-(k,q))-f(-\tilde{E}_+(k,q))\right],\\ \Delta(q,h_v)=-\frac{U_s}{\mathcal{V}}\sum_k\frac{\Delta(q,h_v)}{2\sqrt{E_2^2(k,q)+\Delta^2(q,h_v)}}[f(\tilde{E}_+(k,q))-f(\tilde{E}_-(k,q))].\end{cases} \quad \text{(R2)}$$

Note that here $f(E)$ is the Fermi-Dirac distribution. **Compared to Eq. (3) in the main text, it can be found that the first line of Eq. (R2) has corrected the self-consistent expression for h_v where the occupation difference between two valley bands $E_{k,\tau}$ is just replaced by the occupation difference between two Bogoliubov quasiparticle bands $\tilde{E}_-(k,q)$ and $-\tilde{E}_+(k,q)$.** Once the superconducting order parameter Δ becomes zero (i.e., the normal phase), these self-consistent equations for h_v in Eq. (R2) and Eq. (3) can be verified to be the same, and the physical picture just returns to Fig. 1(a). Especially, as Δ becomes very large, the Bogoliubov quasiparticle band $\tilde{E}_-(k,q)=E_1(k,q)-\sqrt{E_2^2(k,q)+\Delta^2}$ will be totally negative while $\tilde{E}_+(k,q)=E_1(k,q)+\sqrt{E_2^2(k,q)+\Delta^2}$ will be totally positive. This indicates the summation of $\sum_k f(\tilde{E}_-(k,q))$ and $-\sum_k f(-\tilde{E}_+(k,q))$ will be exactly canceled, resulting a zero h_v. This phenomenon directly reflects that the formation of superconducting Cooper pairs will suppress the valley polarization.

Restricting to the single-q order parameter, the supercurrent $J_s(q)$ is approximately proportional to $|\Delta|^2 q$ near the superconducting phase transition [PNAS **119**, e2119548119

(2022)]. In view of this, to investigate the effect of supercurrents j_s on valley polarizations, we consider a fixed non-zero order parameter Δ and focus on the effect of q on $h_v(\Delta, q)$. Analogous to the analysis of Appendix. A in the main text, we set q as a small quantity, neglecting the self-consistent manner and perform a Taylor expansion for the right part of the first-line equation in Eq. (R2):

$$h_v(\Delta, q) \approx h_v(\Delta, q=0) + \beta(\Delta, q=0)q + O(q^2) \tag{R3}$$

where the first-order expansion coefficient $\beta(\Delta, q=0)$ is derived as:

$$\begin{aligned}\beta(\Delta, q=0) &= \frac{U_v}{2\mathcal{V}} \sum_k \left[f'(\tilde{E}_-(k, q=0)) \frac{\partial \tilde{E}_-(k,q)}{\partial q}\bigg|_{q=0} + f'(\tilde{E}_+(k, q=0)) \frac{\partial \tilde{E}_+(k,q)}{\partial q}\bigg|_{q=0} \right] \\ &= \frac{U_v}{2\mathcal{V}} \sum_k [f'(\tilde{E}_+(k, q=0)) + f'(\tilde{E}_-(k, q=0))] \epsilon'_{k,+}\end{aligned} \tag{R4}$$

In Eq. (R4), we can find the the first-order expansion coefficient $\beta(\Delta, q=0)$ is still directly related to the energy band dispersion $\epsilon'_{k,+}$, which is somehow similar to the linear expansion of electric voltage in Eq. (A.7) of the main text. Especially, when the valley bands preserve intravalley inversion symmetry: $\epsilon_{k,\tau} = \epsilon_{-k,\tau}$, the summation in Eq. (R4) will automatically be canceled, indicating that the finite Cooper-pair momentum $2q$ is uneasy to influence h_v. In short, Eq. (R4) demonstrates a relation where the valley polarization is approximately proportional to the finite Cooper-pair momentum $2q$ and also the corresponding supercurrent $j_s \propto q$.

The similarity between the finite-momentum-induced valley polarization modulation and the voltage-induced valley polarization modulation can be also elucidated based on the BdG Hamiltonian. Performing the Taylor expansion of q, the original BdG Hamiltonian $H(q)$ can be rewritten as:

$$\begin{aligned} H(q) &= \sum_k (c^\dagger_{k+q,+}, c_{-k+q,-}) \begin{pmatrix} E_{k+q,+} & -\Delta(q) \\ -\Delta(q) & -E_{-k+q,-} \end{pmatrix} \begin{pmatrix} c_{k+q,+} \\ c^\dagger_{-k+q,-} \end{pmatrix} \\ &= \sum_k (c^\dagger_{k+q,+}, c_{-k+q,-}), \begin{pmatrix} \epsilon_{k+q,+} - \tilde{\mu} - h_v & -\Delta(q) \\ -\Delta(q) & -\epsilon_{k-q,+} + \tilde{\mu} - h_v \end{pmatrix} \begin{pmatrix} c_{k+q,+} \\ c^\dagger_{-k+q,-} \end{pmatrix} \\ &\approx \sum_{k,\tau} (c^\dagger_{k+q,+}, c_{-k+q,-}), \begin{pmatrix} \epsilon_{k,+} + \epsilon'_{k,+}q - \tilde{\mu} - h_v & -\Delta(q) \\ -\Delta(q) & -\epsilon_{k,+} + \epsilon'_{k,+}q + \tilde{\mu} - h_v \end{pmatrix} \begin{pmatrix} c_{k+q,+} \\ c^\dagger_{-k+q,-} \end{pmatrix}. \end{aligned} \tag{R5}$$

In Eq. (R5), although the finite Cooper-pair momentum does not induce a non-equilibrium electron distribution similar to Fig. 1(a) in the main text, it effectively alters the band structure by an energy shift $\epsilon'_{k,+}q$, which still depends on the sign of band dispersions. Taking

1D effective valley bands shown in Fig. 1(a) as an example, in Fig. R2, we schematically demonstrate the effect of this energy shift. In Fig. R2(a), the K valley band $E_{k,+} = \epsilon_{k,+} - \tilde{\mu} - h_v$ (red color) and K' valley band $E_{k,-} = \epsilon_{k,-} - \tilde{\mu} + h_v$ (blue color) are respectively plotted with a finite valley splitting $h_v > 0$. In Fig. R2(b), we convert the K' valley band $E_{k,-}$ into $-E_{-k,-}$ corresponding to the BdG transformation in Eq. (R5). By introducing a finite superconducting order parameter $\Delta \neq 0$, the superconducting gap will open, and the K and K' valley bands are recombined into two Bogoliubov quasiparticle bands $\tilde{E}_+(k)$ (blue color) and $\tilde{E}_-(k)$ (red color). According to Eq. (R2), the valley polarization is now related to the occupation difference between $\sum_k f(\tilde{E}_-(k))$ and $\sum_k f(-\tilde{E}_+(k))$. Especially, considering a contribution of the small momentum q, the energy shift $\epsilon'_{k,+}q$ will break the alignment of right and left parts of BdG bands. **See Fig. R2(d), a finite momentum q respectively induces downward and upward energy shift (purple arrows) around right and left crossing points between $E_{k,+}$ and $E_{-k,-}$.** When valley bands possess intravalley inversion symmetry, the downward and upward energy shifts should be equal and the occupations on each Bogoliubov quasiparticle band $\tilde{E}_-(k,q)$ and $-\tilde{E}_+(k,q)$ are approximately unchanged, also making valley polariztions still. **Conversely, when intravalley inversion symmetry has been broken, the unequal band dispersions indicate opposing energy shifts cannot be equal, and the occupations on each Bogoliubov quasiparticle band $\tilde{E}_-(k,q)$ and $-\tilde{E}_+(k,q)$ can be changed. Moreover, the variations of occupations on two Bogoliubov quasiparticle bands may also not be offset [e.g., Fig. R2(d)], thereby modulating h_v based on Eq. (R2).**

In summary, we demonstrate the rationality of our theoretical framework from two perspectives. First, from a counterfactual perspective, we show that if the system were driven by an electric current across the intersection point in Fig. 1 while remaining in the normal phase, such a normal phase would be inherently unstable. This judgement is largely independent of discontinuity for valley polarizations in normal phases and superconducting phases. Second, we show that even if the physical picture presented in Fig. 1 breaks down in the superconducting regime, a supercurrent can continue to induce a modulation of valley polarization similar to the normal electric current. The presented theory in Fig. 1 of our manuscript focuses on demonstrating the determination of the critical currents from the normal phase to the superconducting phase.

In the revised manuscript, we revised the Fig. 1 and Fig. 3, and added some explanations in 2nd, 3rd and 4th paragraphs of Page 7 to illustrate the logic of our theory to determine the actual critical currents. We also add a new Appendix (Appendix D) with a new figure (Fig. 8) to discuss the supercurrent-induced valley polarization modulations.

Comment **2**:

Does the mean-field model of Eq. (6) possibly combined with (1,2) contain coupling between VP and supercurrent in equilibrium current-carrying state? This would be useful to evaluate and discuss in the text.

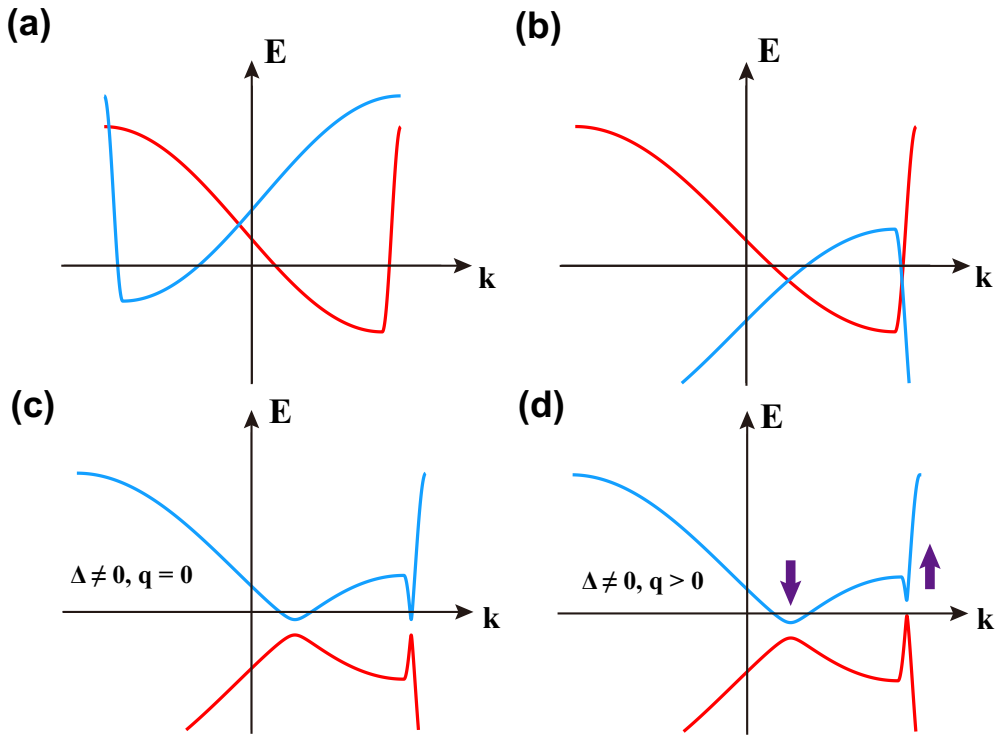

FIG. R2: (a) The schematic diagram for 1D effective valley bands $E_{k,+}$ (red color) and $E_{k,-}$ (blue color) with a finite valley splitting $h_v > 0$. (b) The schematic diagram for K band $E_{k,+}$ (red color) and K' band $-E_{-k,-}$ (blue color) based on the BdG transformation. (c) The schematic diagram for Bogoliubov quasiparticle bands $\tilde{E}_+(k)$ (blue color) and $\tilde{E}_-(k)$ (red color) with a fixed order parameter $\Delta \neq 0$. (c) The schematic diagram for Bogoliubov quasiparticle bands $\tilde{E}_+(k,q)$ (blue color) and $\tilde{E}_-(k,q)$ (red color) with a fixed order parameter $\Delta \neq 0$ and a finite momentum $q > 0$. The purple arrows indicate band shifts, depending on band dispersions of $E_{k,+}$.

Reply: We thank the referee for the insightful suggestions. In the reply to Comment 1, we have illustrated the coupling between VP and the supercurrent in the equilibrium current-carrying state based on a mean-field approximation. We will also add these discussions as a new Appendix (Appendix D) of the revised manuscript.

Comment **3**:

Estimates for the values of the α_{+-} coefficients in Eqs. (4,5) in some more realistic system would be useful. It is currently not easy to see that the values used in calculations are in a regime that is similar to an experimental system. Some values are mentioned in the discussion. Are the figures calculated with parameters that are similar in relative sizes to those required for the magnetization switching in eg. TBG or trilayer?

Reply: We thank the referee for the helpful suggestions. In our work, for the sake of computational simplicity, **we employ an effective 1D model (see details in Sec. 2.3) to qualitatively illustrate the modulation of valley polarization by the applied**

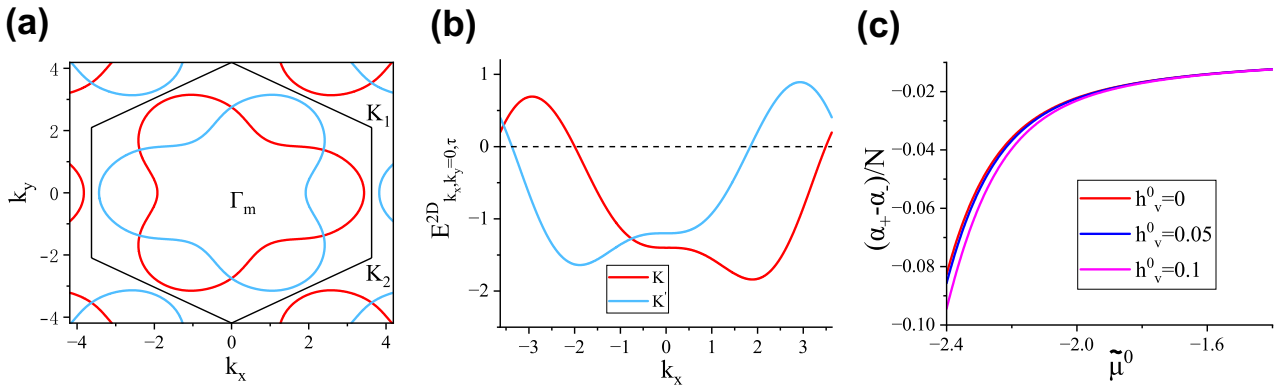

FIG. R3: (a) The trigonally-warped Fermi surfaces of $H_\tau^{2D}(k_x, k_y)$ for effective TBG bands with $t_1 = 1, t_2 = 0.05, t_2' = 0.2$, $h_v = 0$ and $\mu = -1.4$. The red and blue Fermi surfaces denote K and K' valley, respectively. The hexagonal frame mark the moiré Brillouin zone. Note that k_x and k_y are in the units of L_M^{-1}. Here L_M is the moiré lattice constant and be set to $L_M = 1$ in calculations. (b) The 1D effective valley bands of $E^{2D}_{k_x,k_y=0,\tau}$ of H_τ^{2D} with a finite valley splitting field $h_v = 0.1$. (c) The change of modulation coefficient $(\alpha_+ - \alpha_-)/N$ versus the initial chemical potential $\tilde{\mu}^0$ for several initial valley splitting field h_v^0. Here the coefficient α_τ is in the unit of $h/2et_1$.

current, as well as the corresponding modulation of the superconducting critical current. Similar toy model has been also used in previous study [Phys. Rev. Lett. **125**, 226401 (2020)]. Although a direct quantitative comparison between our 1D effective model and the actual 2D bands of twisted graphene systems is hard, we emphasis the effective model has captured the main feature of the problem: the broken intravalley inversion symmetry. Our calculations has also demonstrated the physical phenomena qualitative agreement with the experimental observations [Nat. Phys. **18**, 1221 (2022)]. The experiment and our theoretical calculations both show that varying carrier density and the external magnetic field can significantly influence the efficiency of superconducting diode effect, even drive the system into an extreme nonreciprocal SDE.

On the other hand, through some rough estimations, it can be also found the magnitude of our calculated results from our 1D effective model is basically consistent with the experimental observations. Considering a typical narrow bandwidth 10 meV of flat bands for twisted graphene systems [Phys. Rev. B **104**, L121116 (2021)], we estimate that the energy unit and current unit used in calculations are respectively about $t = 2.5$ meV and $\frac{e}{h}t \approx 96.6$ nA (see Discussions and conclusion of our manuscript). Based on this, we estimate that the amplitudes of actual critical currents j_c in Fig. 4(a) for extreme nonreciprocal SDE is about 20 nA, which is aligned with the corresponding amplitude in experiment measurements [see Fig. 2g in Nat. Phys. **18**, 1221 (2022)]. Moreover, the normal currents arranging from several nA to tens of nA is experimentally confirmed to be able to modulate or even switch magnetizations in twisted bilayer graphene [Science **365**, 605 (2019), Science **367**, 900 (2020)], which are also consistent with the magnitudes of currents in our theoretical calculations.

It should be also noted that in some more realistic system, the parameters for $\alpha_\pm$ are

likewise significant. To estimate the values of $\alpha_{\pm}$, we here use a more realistic tight-binding Hamiltonian on the honeycomb lattice with (p_x, p_y) orbitals, which are often used to simulate the four lowest moiré bands of twisted bilayer graphene [Phys. Rev. B **98**, 045103 (2018), Phys. Rev. X **8**, 031087 (2018), Phys. Rev. Lett. **130**, 266003 (2023)]. It is written as:

$$H_{\tau}^{2D} = \sum_{\langle ij \rangle} t_1 c_{i,\tau}^{\dagger} c_{j,\tau} + \sum_{\langle ij \rangle'} (t_2 - i\tau t_2') c_{i,\tau}^{\dagger} c_{j,\tau} + \text{H.c.} - \sum_{i,\tau} (\tilde{\mu} + \tau h_v) c_{i,\tau}^{\dagger} c_{i,\tau}. \tag{R6}$$

where $\langle ij \rangle$ denotes the nearest-neighbor hopping terms with the hopping energy t_1, $\langle ij \rangle'$ denotes the fifth nearest-neighbor hopping terms with the hopping energy t_2 and t_2'. $c_{i,\tau}^{\dagger}$ and $c_{i,\tau}$ respectively denote the creation and annihilation operator for the electron at the lattice site i with $p_x + i\tau p_y$ orbital ($\tau = \pm$ represent K and K' valley). Similar to the procedure in our main text, we choose t_1 as the energy unit ($t_1 = 1$), and set $t_2 = 0.05t_1$, $t_2^{'} = 0.2t_1$ according to the Reference [Phys. Rev. Lett. **130**, 266003 (2023)]. Usually, for magic-angle TBG, the hopping energy of t_1 corresponds to 4 meV. Note that t_2' characterizes the trigonal warping effect, as is shown by the triangular-shaped Fermi surfaces of $H_{\tau}^{2D}(k_x, k_y)$ in Fig. R3(a). It is evident for TBG bands to break the intravalley inversion symmetry.

For simplicity, we also fix $k_y = 0$ and reduce the 2D energy bands of TBG as an 1D energy band. In Fig. R3(b), we plot two valley bands $E_{k_x,k_y=0,\tau}^{2D}$ near the Fermi surface also with a initial finite valley splitting $h_v = 0.1t_1$. Similar to Fig. 1(a), we can see they both exhibit an evident band asymmetry: $E_{k_x,k_y=0,\tau}^{2D} \neq E_{-k_x,k_y=0,\tau}^{2D}$. We use Eq. (A.7) to calculate the modulation coefficient $(\alpha_+ - \alpha_-)/N$ of the 1D energy band $E_{k_x,k_y=0,\tau}^{2D}$ versus the initial chemical potential $\tilde{\mu}^0$ for several initial valley splitting field h_v^0. Here $T = 0.1t_1$ (thermal energy) and $N = 2000$ corresponds to the number of discrete k_x points. It can be found that $(\alpha_+ - \alpha_-)/N$ has demonstrated relatively large values at some chemical potentials.

In the revised manuscript, we add some statements in the section 'Discussions and conclusion' to emphasis the correspondence between our theoretical calculations and experimental observations. We also add some discussions in Appendix. E with a new figure Fig. 9, to demonstrate the estimation of $\alpha_{\pm}$ in a more realistic tight-binding model.